Dramatic enhancement of the stability of rare-earth metal complexes with α-methyl substituted N,N-dimethylbenzylamine ligands

Alex R. Petrov [a], Oliver Thomas [a], Klaus Harms [a], Konstantin A. Rufanov [a,b], Jörg Sundermeyer [a,*]

[a] Fachbereich Chemie der Philipps-Universität Marburg, Hans-Meerwein-Strasse, 35032 Marburg, Germany
[b] Department of Chemistry, M.V. Lomonosov State University of Moscow, 19992, Moscow, Russian Federation

ARTICLE INFO

ABSTRACT

Stepwise substitution of benzylic CH_2 protons in ortho-metallated N,N-dimethylbenzylamine (dmba) ligands leads to chiral ortho-metallated N,N,α-trimethylbenzylamine (tmba) and cumyl-N,N-dimethyl-amine (cuda) ligands. These larger ligands with less or no acidic protons in benzylic position prove to stabilize some of those homoleptic tris-aryls of the larger (middle) and largest (early) rare-earth metal cations, for which such tris-aryl or tris-dmba complexes could not be synthesized so far. The syntheses, characterization and crystal structures of [Li(cuda)], [(tmba)$_2$Lu(μ-Cl)]$_2$ (**1**), [(tmba)$_2$Y(μ-Cl)]$_2$ (**2**), [Y(tmba)$_3$] (**3**), [Dy(tmba)$_3$] (**4**), [Nd(tmba)$_3$] (**5**), [Sm(tmba)$_3$] (**6**), and [Sm(cuda)$_3$] (**7**) are reported, trends in complex stability are discussed.

© 2010 Elsevier B.V. All rights reserved.

1. Introduction

The bidentate monoanionic ortho-metallated N,N-dimethylbenzylamine ligand (dmba) found broad application in the organometallic chemistry. Complexes with this ligand motif are known for almost every transition metal. This ligand may be introduced using the aryllithium reagent 2-lithio-N,N-dimethylbenzylamine Li(dmba) which itself is conveniently prepared by ortho-directed lithiation of N,N-dimethylbenzylamine [1]. This chelate ligand can perfectly provide kinetic stabilization of its metal aryl complexes by the strongly σ-donating dimethylamino group. Homoleptic tris-aryles [Ln(dmba)$_3$] are known for late rare-earth metals with small ionic radii (Er, Yb and Lu [2], Sc [3], Y [4]). Furthermore it was reported that due to not identified decomposition paths no such complexes with larger cations of the early or middle lanthanides exist [2].
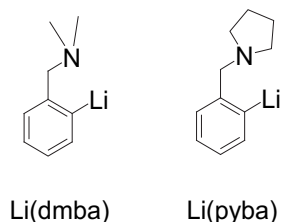
Recently we reported a reinvestigation of the reactions of ortho-lithiated N,N-dimethylbenzylamine [Li(dmba)] and N-benzylpyr-rrolidine [Li(pyba)] ligands with different lanthanide and group 3 metal complexes (Scheme 1).

Our observations denote the crucial role of coordinated solvent in the lanthanide precursors [LnCl$_3$(solv)$_n$] on the formation of the transmetallated products. The use of [NdCl$_3$(dme)] or [GdCl$_3$(dme)$_2$] instead of their THF-solvated pendants and a slight modification of the ligand framework (dmba → pyba) allowed the isolation and XRD structural characterization of highly air-sensitive, crystalline lithium tetrakis-aryl-ate complexes of early and middle lanthanide metals, namely Li[Nd(pyba)$_4$] and Li[Gd(tmba)$_4$] (Scheme 2) [5].

The existence of tris-dmba complexes only for smaller (or late) lanthanides (Er–Lu) and the smaller group 3 metals Y and Sc indicates that for stabilization of such homoleptic aryls of early (La–Sm) and middle (Eu–Ho) lanthanides further modification of the dmba ligand is required.

In this context it is interesting to note, that deprotonation of N,N-dimethylbenzylamine with n-BuLi in ether takes place exclusively at the ortho-position of the phenyl ring as a result of a kinetically as well as thermodynamically controlled reaction. When alkylsodium compounds (e.g. n-BuNa or n-AmNa) suspended in hexane are used, deprotonation of N,N-dimethylbenzylamine under kinetic control occurs at the ortho-position (Scheme 3), however, the ortho-sodio aryl derivative is unstable and isomerizes into thermodynamically more stable benzyl or α-sodio species within 20 h, respectively [6]. The softer metal cation Na$^+$ (vs. Li$^+$) tends to better stabilize the softer benzyl (and not aryl) carbanion. The preference of even softer

* Corresponding author. Tel.: +49 6421 28 25693; fax: +49 6421 28 28917.
E-mail address: jsu@chemie.uni-marburg.de (J. Sundermeyer).

Scheme 1. Earlier studied benzylamine-derived ligands.

Ln = Nd (R = -(CH$_2$)$_4$-),
Gd (R = Me).

Scheme 2. Synthesis of the lithium ate-complexes Li[Nd(pyba)$_4$] and Li[Gd(dimba)$_4$].

cation K$^+$ to interact with benzylic carbanions in highly aggregated structures is well documented by XRD structural analyses of [PhCH$_2$K(pmdta)]$_\infty$ [7], [PhCH$_2$K(thf)]$_\infty$ [8], [Ph(Me$_3$Si)$_2$CK]$_\infty$ [9] and [Me$_2$NC$_6$H$_4$CHSiMe$_3$K(thf)]$_\infty$ [10].

On the other hand the α-lithio derivative being prepared from the α-sodio compound by metathesis with lithium bromide is stable at 25–30 °C for at least 24 h. At higher temperatures (45 °C/45 h), this species slowly isomerizes forming the thermodynamically more stable *ortho*-lithio derivative. We anticipated that the availability of acidic benzylic protons would strongly influence the stability of the primary products with larger and softer early rare-earth metals obtained via transmetallation with Li(dmba). Therefore substitution of benzylic protons by one or two methyl groups should have a strong impact on complex stability of larger cations.

Here we report our achievements in organometallic chemistry of early, middle and late lanthanide complexes with *mono*- and *bis*-α-methyl substituted dmba ligands.

1.1. Synthesis of aryllithium reagents Li(tmba) and Li(cuda)

The α-methyl- and α,α-dimethyl substituted benzylamine precursors are *N,N,α*-trimethyl-benzylamine (tmba)H and cumyl-*N,N*-dimethylamine (cuda)H (Scheme 4). Both amines were synthesized according to the literature procedures from (*S*)-phenylethylamine and *tert*-cumylamine [11] by the standard protocol for methylation under *Eschweiler-Clark* conditions [12].

The synthesis and properties of aryllithium reagent Li(tmba) were first reported in 2004 by van Koten et al. [13]. It was shown that the appearance, reactivity and physicochemical properties of *ortho*-lithiated racemic and enantiopure amine differ dramatically. Therefore, the metallation was investigated with (*S*)-phenylethyl-amine instead of the racemate. The synthesis of the aryllithium reagent was performed using *tert*-BuLi as deprotonating agent in pentane at room temperature [14].

The second aryllithium reagent – *ortho*-lithiated cumyl-*N,N*-dimethylamine, Li(cuda) (**2**) – was previously generated *in situ* by
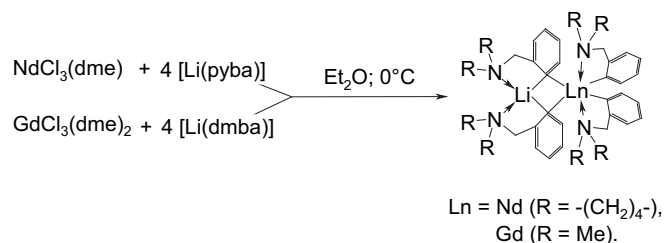
metallation of (*o*-BrC$_6$H$_4$)C(Me)$_2$NMe$_2$ with *n*-BuLi and further used for a following reaction in boron chemistry. No isolation or characterization of the compound was attempted [15].

We have synthesized and completely characterized Li(cuda) by deprotonation of *N,N*-dimethyl-cumylamine with *tert*-BuLi in multigram scale. The product shows higher solubility in ethereal and aliphatic solvents than Li(tmba). The isolation of this lithium reagent was achieved by storing its pentane solution at −30 °C. The product was isolated in 55% yield. Crystallisation from ether leads to an etherate of the composition Li(cuda) × ½Et$_2$O. Attempts to remove the coordinated ether molecule by drying in vacuum at 10^{-2} mbar/20 °C were unsuccessful. This stable etherate could also be used as a convenient precursor. In the ^{1}H NMR spectrum of Li (cuda), sharp resonances for NMe$_2$ and CMe$_2$ at 2.16 and 1.35 ppm respectively were observed. The fluxional behavior of the cuda ligands in those Li etherates is reflected by significant broadening of *Me*$_2$C and *Me*$_2$N group resonances (1.42 and 1.76 ppm respectively).

1.2. Rare-earth complexes with tmba ligand

In first experiments on transmetallation with the aryllithium reagent Li(tmba), the synthesis of the homoleptic lutetium complex [Lu(tmba)$_3$] was attempted. The salt metathesis reaction of three equiv. of this aryllithium reagent with one equiv. [LuCl$_3$(thf)$_3$] [16] did not lead to expected [Lu(tmba)$_3$], the homologue of [Lu (dmba)$_3$]. Cooling the hexane extract of non-volatile reaction products leads to precipitation of a crystalline solid, that was identified as [(tmba)$_2$Lu(μ-Cl)]$_2$ (**1**). This is the first heteroleptic *bis*-aryl-chloro lanthanide complex in this series. Even prolonged reaction times (24 d at 20 °C) did not result in the substitution of the third chlorine atom in this complex. The composition of **1** was also confirmed by elemental analysis (Fig. 1). The ^{1}H NMR spectrum of **1** reveals three broad resonances for diastereotopic methyl groups of Me$_2$N and for C(H)Me suggesting a cis coordination of both ligands in an octahedral chlorine bridged dinuclear complex,
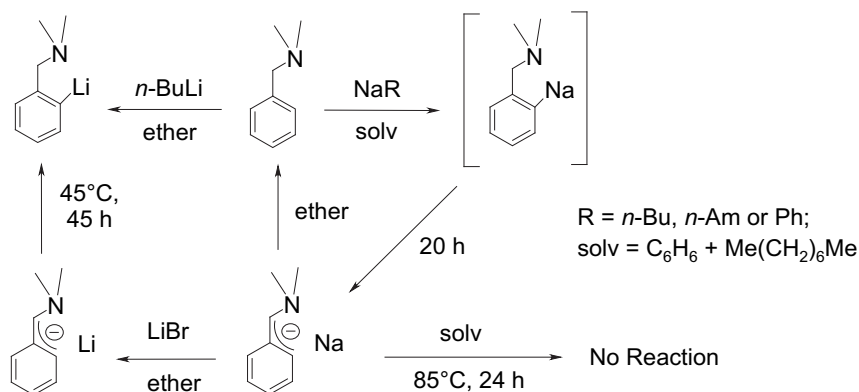
Scheme 3. Deprotonation of *N,N*-dimethylbenzylamine with lithio- and sodio-organyls and their following transmetallation/isomerization reactions.
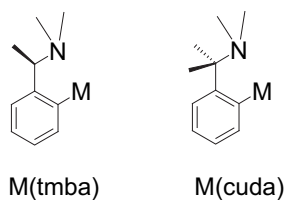
Scheme 4. α-Methyl substituted benzylamine-type ligands N,N,α-trimethylbenzyl-amine (tmba)H and cumyl-N,N-dimethylamine (cuda)H.

Scheme 5. Reactivity of Li(tmba) with late and middle rare-earth metal halides.

which was later confirmed by XRD analysis to be also the solid state molecular structure (Fig. 1).

Introduction of only one methyl substituent at the benzylic position results in a dramatic increase of the steric bulk of the ligand which allowed the isolation of so far unknown chloro–aryl complexes. With respect to their potential as convenient precursors for the synthesis of other heteroleptic lanthanide complexes, it was of interest to investigate, whether other complexes with a bis-aryl-chloro substitution pattern would be accessible. Indeed, salt metathesis reaction of [YCl$_3$(dme)$_2$] with 2 equiv. of Li(tmba) leads selectively to heteroleptic [(tmba)$_2$Y(μ-Cl)]$_2$ (**2**); whereas with 3 equiv. of the reagent, homoleptic [Y(tmba)$_3$] (**3**) can easily be prepared (Scheme 5).

Complex **2** crystallizes from ether with additional solvent molecules (**2** × 1.33Et$_2$O) as shown by XRD analysis. The molecular structures of the heteroleptic complexes **1** and **2** are depicted in Fig. 1. These compounds crystallize in the orthorhombic P2$_1$2$_1$2$_1$ (Z = 16) and the cubic space groups I23 (Z = 6) respectively. Whereas in the structure of **2** one centrosymmetric molecule was observed, four independent asymmetric dimeric molecules were found in the structure of lutetium complex **1**, one of them is depicted in Fig. 1.

In these dimeric complexes **1** and **2**, the metal centers adopt highly distorted octahedral configurations with bridging chlorine atoms. The bond lengths and angles in structure of **1** vary in very broad intervals; selected bond lengths and angles for **1** and **2** are given in Table 1. In the unit cell of **2**, disordered ether molecules were observed.

Analogous reaction of [DyCl$_3$(dme)$_2$] with Li(tmba) in a 1:3 ratio also leads to formation of [Dy(tmba)$_3$] (**4**) in a yield of 83% (Scheme 5). Yellowish **4** and colorless **3** were isolated by crystallization from ether and hexane respectively. Both complexes possess a high thermal stability and show high solubility in aromatic solvents.

The homoleptic yttrium complex **3** crystallizes in the monoclinic space group P2$_1$ with two independent molecules in the unit cell. The molecular structure is presented in Fig. 2, selected bond lengths and angles in Table 2.
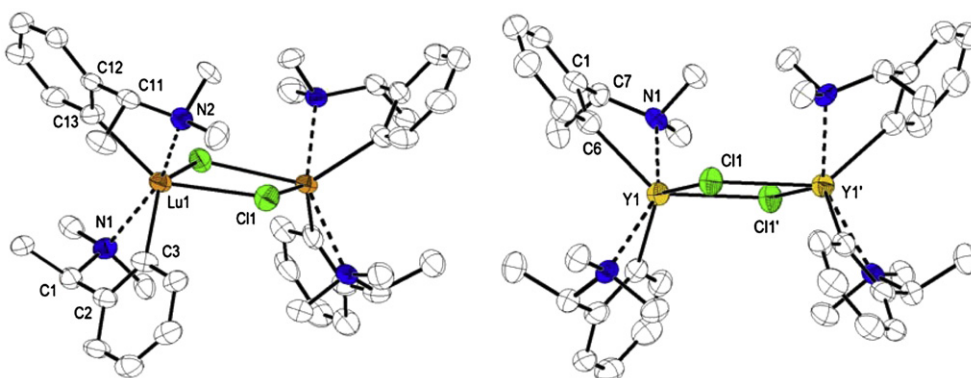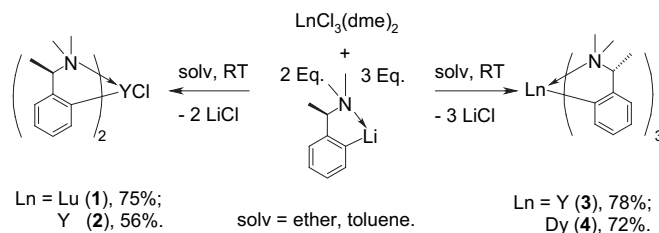
The molecular architecture is similar to the pattern found in the earlier described homoleptic dmba complexes of late lanthanides and yttrium. Differences within the independent molecules arise from a different pattern of shorter and longer Ln–C and Ln–N bonds. Comparison with the related yttrium complex [Y(dmba)$_3$] reveals similarities in the values for angles, but some differences in the Y–N and Y–C bond lengths. In general all Y–N bond lengths are slightly longer by ca. 0.5 Å for **3** than in complex [Y(dmba)$_3$], while the three Y–C bonds of both independent molecules of **3** are shorter than in reference complex [Y(dmba)$_3$] (Y–C: 2.504(3), 2.475(2), 2.479(4) Å).

The YC$_3$ coordination motif is close to trigonal planar. Deviation of the metal center from the CCC plane is larger (0.457(1) and 0.350(1) Å for both independent molecules), the sum of C$_{Ar}$–Y–C$_{Ar}$ angles smaller (349.5(8) and 353.7(9)°) compared to sterically less crowded [Y(dmba)$_3$].

The chiral tmba ligand coordinated at a metal center exhibits at least two conformations in the solid state: The methyl substituent is orientated either nearly orthogonal to the aromatic ring plane (out-of-plane conformation, φ → 90°, Scheme 6) or it is oriented nearly coplanar to the aromatic ring (in-plane, φ → 0°).

According to this definition, the independent molecules of [Y(tmba)$_3$] **3** have different conformations of the tmba ligands. One molecule in the unit cell has mixed in-in-out tmba ligand conformations with the φ-angles of 10.4(7), 8.1(6) and 82.6(4)° respectively. The other independent molecule has out-out-in-conformations with the φ-angles of 82.3(5), 87.5(7) and 8.9(6)° respectively.

Unlike all complexes crystallographically characterized previously, [Dy(tmba)$_3$] (**4**) featuring a slightly larger Dy^{3+} metal cation crystallizes in the orthorhombic space group P2$_1$2$_1$2$_1$ (Fig. 3). Again two independent molecules are found in the unit cell. The selected bond lengths and angles are given in Table 2.

The Dy–C bond lengths vary from 2.450(8) to 2.518(7) Å. Unexpectedly they are significantly longer than those Dy–C(sp^3) bonds in sterically demanding silyl- and disilylmethanide complexes [{η^5-Me$_4$C$_5$SiMe$_3$}-Dy(CH$_2$SiMe$_3$)$_2$(thf)] (Dy–C: 2.410(3), 2.373(2) Å) [17] and [{η^5,η^5-C$_5$H$_4$SiMe$_2$Flu}DyCH(SiMe$_3$)$_2$] (Dy–C: 2.364(9) Å) [18].

Fig. 1. The molecular structure of the complexes [(tmba)$_2$Lu(μ-Cl)]$_2$ (**1**) and [(tmba)$_2$Y(μ-Cl)]$_2$ (**2**). All hydrogen atoms have been omitted for clarity.

Table 1
Selected bond lengths (Å) and angles (°) for the complexes [(tmba)$_2$M(μ-Cl)]$_2$ (**1**) and (**2**).

	1 (M = Lu)	**2** (M = Y)
M–N	2.456(10)–2.552(10)	2.500(5)
M–C	2.348(13)–2.400(11)	2.430(7)
M–Cl	2.622(3)–2.717(3)	2.733(1)
C$_A$–M–C$_B$	111.8(4)–123.4(5)	121.5(3)
N$_A$–M–N$_B$	141.7(4)–166.3(3)	148.0(2)
Cl$_A$–M–Cl$_B$	76.5(1)–78.9(1)	76.9(1)
M$_A$–Cl–M$_B$	100.9(1)–104.1(1)	103.1(1)

Table 2
Selected bond lengths (Å) and angles (°) for homoleptic [M(tmba)$_3$] complexes **3** and **4**.

	3 (M = Y)		**4** (M = Dy)	
	Molecule 1	Molecule 2	Molecule 1	Molecule 2
M–N1	2.666(6)	2.587(7)	2.548(7)	2.611(7)
M–N2	2.580(7)	2.599(7)	2.666(9)	2.570(7)
M–N3	2.569(7)	2.568(8)	2.566(8)	2.606(8)
M–C1	2.435(7)	2.422(9)	2.518(7)	2.453(7)
M–C10	2.459(8)	2.468(10)	2.450(11)	2.508(9)
M–C19	2.468(8)	2.471(8)	2.450(8)	2.483(8)
C1–M–C10	124.0(2)	99.4(3)	134.1(3)	124.7(3)
C10–M–C19	121.7(3)	132.6(3)	99.5(3)	134.4(3)
C1–M–C19	103.8(3)	121.7(3)	116.2(3)	94.9(3)
∑(C$_A$–M–C$_B$)	349.5(8)	353.7(9)	349.8(9)	354.0(9)
N1–M–N2	125.2(2)	94.1(2)	116.8(3)	140.3(2)
N2–M–N3	144.1(2)	119.7(2)	88.6(3)	117.4(2)
N1–M–N3	87.3(2)	140.0(3)	151.1(1)	94.1(1)
∑(N$_A$–M–N$_B$)	356.6(6)	353.8(7)	356.5(7)	351.8(5)
M⋯CCC[a]	0.457(1)	0.350(1)	0.343(4)	0.447(4)
M⋯NNN[a]	0.255(1)	0.352(1)	0.244(4)	0.408(1)

[a] M⋯CCC and M⋯NNN denote the distance of metal with respect to the plane defined by atoms N1, N2, N3 and C1, C10, C19 respectively.

Conformations of the benzylic methyl substituents of **4** differ from those of **3**. While in **3** the same number of in- and *out-of-plane* conformations was observed, both independent molecules of **4** have predominantly *out-of-plane* conformations in the solid state: **4A** (φ-angles of 85.5(5), 84.9(4) and 89.2(8)°), **4B** (φ-angles of 86.0 (4), 88.9(7) and 1.4(6)°). Moreover, the angles are closer to the ideal values of 90° and 0° in comparison to compound **3**.

Motivated by this success, reactions of Li(tmba) with early lanthanide trihalides of Nd and Sm were studied. Both reactions started at 0 °C in ether/toluene (1:1, v/v) solvent mixture proceed quickly with formation of light-green (Nd) or deep yellow (Sm) solutions and precipitation of LiCl (Scheme 7). It is essential to work-up at low temperatures (<0 °C), because at ambient temperature reaction mixtures become brown and obviously a decomposition of the initially formed complexes [Nd(tmba)$_3$] (**5**) and [Sm(tmba)$_3$] (**6**) takes place.

Both complexes were isolated by storing their saturated hexane solutions at −30 °C for several days. An acceptable elemental analysis was obtained for both complexes. For the neodymium complex **5** we succeeded to obtain crystals, suitable for X-ray analysis. Similar to dysprosium complex **4**, neodymium complex [Nd(tmba)$_3$] **5** crystallizes in the orthorhombic space group $P2_12_12_1$. The molecular structure is depicted in Fig. 4. One ligand shows disorder with occupancy ratio of 0.603:0.397.

The molecules differ by the conformation of only one of three tmba ligands, the positions of other two ligands and even the position of the metal center in the lattice are identical. This obviously is a result of low conformational barriers and small energetic differences in the ground states between *in-* and *out-*conformations in these complexes.

1.3. Rare-earth complexes with cuda ligand

Finally, we have began to study the reactivity of the cuda ligand. With additional bulk provided by the second α-methyl substituent and absence of any benzyl protons the obvious target was to stabilize homoleptic middle and early rare-earth *tris*-aryl complexes with the cuda ligand.

The first experiment to react [LaCl$_3$(dme)] with three equivalents of Li(cuda) in ether gave a colorless, crystalline solid. XRD analysis revealed a binuclear etherate of Li(cuda). Both, ether and DME molecules are coordinated at the ratio of 0.68/0.32. The molecular structure of [Li$_2$(cuda)$_2$(Et$_2$O)$_{0.68}$(dme)$_{0.32}$] is presented in Fig. 5.

In the solid state, the compound adopts an approximately C_2-symmetric, propeller-like structure, in which two lithium atoms are bridged by the *ipso*-carbon atoms of the aryl groups thus forming a nearly planar Li$_2$C$_2$-ring. The Li2 atom is coordinated by Et$_2$O (O1) and DME (O1A, O2A) molecules. The tetrahedral coordination at Li1 is completed by two Me$_2$N groups of the cuda ligand. So far we were
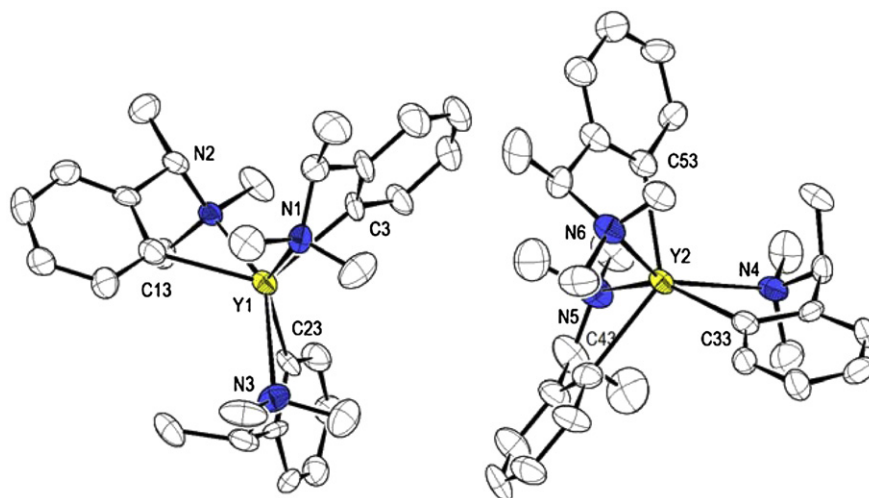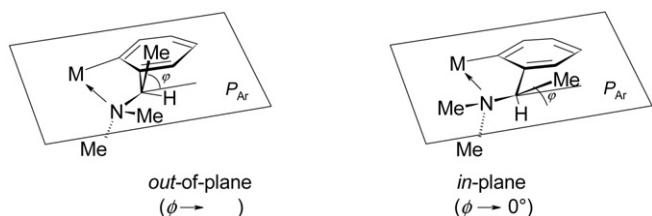

Fig. 2. The molecular structure of the complex [Y(tmba)$_3$] (**3**). All hydrogen atoms have been omitted for clarity.

Scheme 6. The *out-of-* and *in-plane* conformations of the tmba ligand in its complexes. The φ-angle is defined as the angle between the C–Me bond and the aryl plane (P_{Ar}).

Scheme 7. Synthesis of complexes [Nd(tmba)$_3$] (**5**) and [Sm(tmba)$_3$] (**6**).

not able to fully characterize the proposed *tris*-cuda lanthanum complex.

The next plan was the synthesis of samarium complex [Sm(cuda)$_3$] (**7**) starting from [SmCl$_3$(dme)$_2$] and Li(cuda) in ether/toluene mixture (1:1, v/v). As in the case of [Sm(tmba)$_3$] (**6**) the reaction proceeds quickly at 0 °C with formation of deep yellow solution and a precipitation of LiCl (Scheme 8). In this case, no (detectable) decomposition upon warming to ambient temperature takes place. Without any doubt, cuda is a ligand better stabilizing larger rare-earth cations than tmba or dmba, which offers many perspectives in providing stable solutions of rare-earth aryls of larger ionic radii for applications in catalysis or materials chemistry [19].

[Sm(cuda)$_3$] (**7**) is a bright yellow microcrystalline powder stable for several hours to days at ambient temperature. It can be stored at −30 °C without decomposition for at least three months. Good elemental analysis was obtained for this complex. The compound is highly reactive, it decomposes when dissolved in THF forming a colorless solution. Single crystals, suitable for X-ray diffraction, were obtained by crystallization from the saturated diethyl ether solution at −30 °C. The molecular structure of **7** is depicted in Fig. 6.

The complex crystallizes in the monoclinic space group $P2_1/c$ with $Z = 4$. The coordination is similar to those of the late and middle lanthanide tmba complexes and also best described as a highly distorted *pseudo*-octahedral. The Sm–C bond lengths vary from 2.489(5) to 2.550(4) Å; the Sm–N bond lengths from 2.628(3) to 2.709(3) Å. Comparison with neutral mononuclear complexes reveals that the Sm–C bond lengths fall into the range of reported ones in [{o-(o-MeOC$_6$H$_4$)$_2$C$_6$H$_3$}Sm{N(SiHMe$_2$)$_2$}$_2$] [20] (2.483 Å), [(η^5-Me$_5$C$_5$)$_2$SmPh(thf)] [21] (2.511 Å), [(o-C$_4$H$_3$N-C$_6$H$_4$)Sm(η^5-C$_5$Me$_5$)$_2$] [22] (2.527 Å), [{o-Mes$_2$C$_6$H$_3$}Sm(η^8-C$_8$H$_8$)(thf)] (2.529 Å), [(o-(o-MeOC$_6$H$_4$)$_2$C$_6$H$_3$)Sm(η^8-C$_8$H$_8$)(thf)] [23] (2.543 Å), [(o-Mes$_2$C$_6$H$_3$)SmCl$_2$(ImMe)$_2$-(thf)] [24] (2.532 Å), and [(o-Mes$_2$C$_6$H$_3$)SmCp] [25] (2.536 Å).
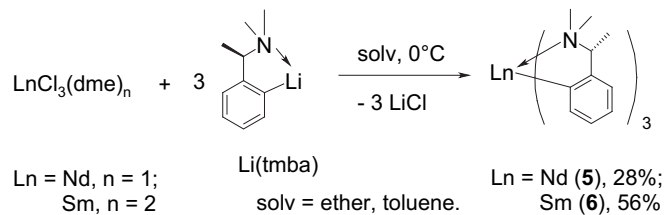
2. Conclusions

The results achieved are summarized in Table 3. The sterically less demanding ligand (dmba) does not stabilize early lanthanide complexes with large ionic radii [LnAr$_3$] (Ln = Ce–Sm, La). The largest rare-earth cation forming homoleptic *tris*-aryl complexes with (dmba) or (pyba) is yttrium followed by the late lanthanide cations (Er^{3+}, Yb^{3+}, Lu^{3+}). On the other hand less bulky dmba and pyba ligands form interesting lithium ate-complexes with the early (Nd) and middle (Gd) lanthanide cations. Stabilization of early homoleptic Ln^{3+} complexes was achieved when benzylic CH$_2$ protons in dmba are substituted by one or two methyl groups (tmba/cuda). A mismatch of cation size and ligand bulk leads either to unstable species of early and middle lanthanides with less crowded ligands, or to incomplete substitution and formation of heteroleptic complex [Ln(tmba)$_2$Cl]. Both, [Y(tmba)$_3$] and [Y(tmba)$_2$Cl] can be synthesized selectively. Up to date, the stabilization of complexes [Ln(tmba)$_3$] with the larger late lanthanides (Er, Tm) or [Ln(cuda)$_3$] with the middle lanthanides (Eu–Ho, Y) remains unverified, but probable. Stabilization of *tris*-aryl complexes of the smaller late lanthanides with sterically demanding cuda ligand is improbable. Ligand size has to match cation size – then stable complexes arise.
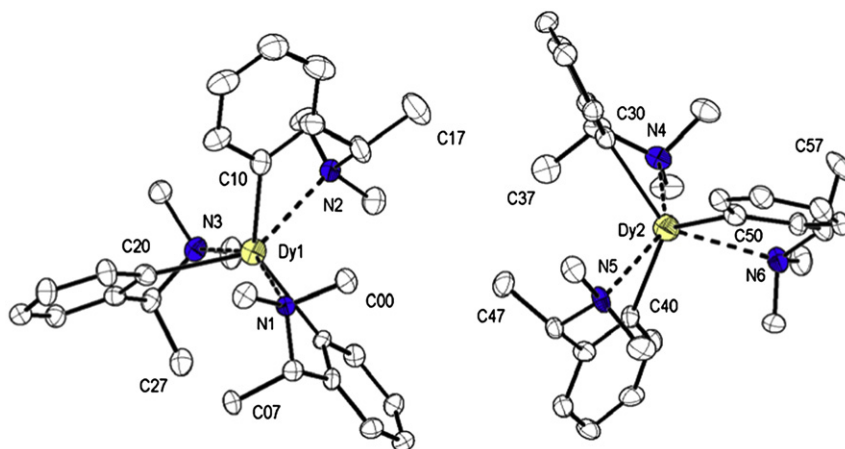
3. Experimental part

Fig. 3. The molecular view of two independent molecules in the complex [Dy(tmba)$_3$] (**4**). All hydrogen atoms have been omitted for clarity.

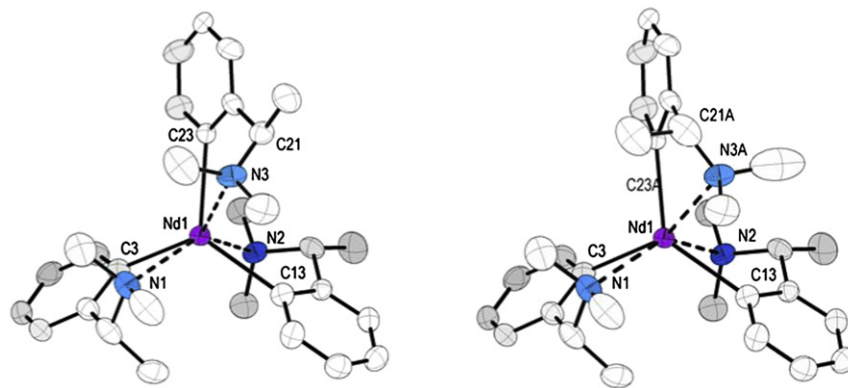**Fig. 4.** The molecular structures of two conformations due to disorder in neodymium complex [Nd(tmba)$_3$] (**5**): *out-in-in*-conformation (left) and *out-in-out*-conformation (right). All hydrogen atoms have been omitted for clarity. Selected bond lengths (Å) and angles (Å): Nd1−N1 2.678(1), Nd1−N2 2.653(1), Nd1−N3 2.750(1), Nd−N3A 2.789(1), Nd−C3 2.565 (5), Nd−C13 2.557(5), Nd−C23 2.589(4), Nd−C23A 2.440(14), N1−Nd1−N2 139.4(1), N2−Nd1−N3 126.6(1), N3−Nd1−N1 89.8(1), N2−Nd1−N3A 111.5(1), N3A−Nd1−N1 103.2(1), C3−Nd1−C13 120.7(2), C13−Nd1−C23 122.7(1), C23−Nd1−C13 106.4(1), C13−Nd1−C23A 130.4(1), C23A−Nd1−C13 101.7(1); for *out-in-in*-conformer (left): ∑(N$_A$−Nd1−N$_B$), 355.8 (3), ∑(C$_A$−Nd1−C$_B$) 349.8(5), Nd1···CCC 0.474(1), Nd1···NNN 0.303(1); for *out-in-out* conformer (right): ∑(N$_A$−Nd1−N$_B$) 354.1(3), ∑(C$_A$−Nd1−C$_B$) 352.8(3), Nd1···CCC 0.384(1), Nd1···NNN 0.364(1).
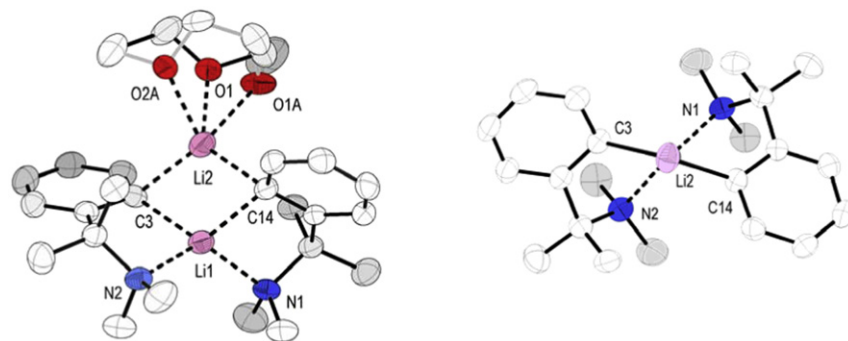
Fig. 5. The molecular structures of [Li$_2$(cuda)$_2$(Et$_2$O)$_{0.68}$(dme)$_{0.32}$]: side view (right) and view along the *pseudo*-C$_2$-axis through Li1···Li2 axis. Hydrogen atoms have been omitted for clarity. In the right picture ether molecules have also been omitted. Selected bond lengths (Å) and angles (°): Li1−C3 2.188(3), Li1−C14 2.207(3), Li2−C3 2.181(4), Li2−C14 2.173(3), Li1−N1 2.120(3), Li1−N2 2.087(3), Li2−O1 1.851(4), Li2−O1A 2.326(7), Li2−O2A 2.105(5), L1−C3−Li2 66.3(1), Li1−C13−Li2 66.1(1), C3−Li1−C13 112.8(1), C3−Li2−C13 114.5(2), N1−Li1−N2 121.3(1).

in the literature: [LnCl$_3$(dme)$_n$] (Ln = Lu, Y, Sm, Dy; n = 2 and Ln = La, Nd; n = 1) [26], PhC(Me)$_2$NH$_2$ [11], (S)-PhCH(Me)NMe$_2$ [13]. Following reagents: formic acid, 37% aq. formaldehyde and *tert*-BuLi (15% in pentane) − were used as supplied (Acros, Aldrich).

Cumyl-N,N-dimethylamine (cuda)H: Cumylamine (5.0 g, 37 mmol) was added to an ice cooled mixture of formic acid (11.1 mL, 0.3 mol, 8 equiv.) and formaldehyde (37%, 13.9 mL, 122 mmol, 3.3 equiv.). The mixture was brought to ambient temperature and heated to 70 °C whereupon an exothermic reaction with gas evolution began. After the vigorous gas evolution dyed out, the reaction mixture was refluxed for 1 h. It was cooled with an ice bath, extracted twice with ether (2 × 30 mL) and was made alkaline by addition of excess of 50% solution of NaOH. The separated organic phase was separated and the aqueous phase was extracted with ether (3 × 50 mL). The combined organic phases were successively dried with Na$_2$SO$_4$ and CaH$_2$ followed by removal of

solvent in vacuum. Compound was purified by vacuum distillation (83 °C/16 mm). A colorless liquid was obtained in 75% yield (4.5 g, 27 mmol). ^{1}H NMR (300.1 MHz, CDCl$_3$): 1.35 (s, 6H, CMe$_2$), 2.16 (s, 6H, NMe$_2$), 7.19 (t, $^3J_{HH}$ = 7.1 Hz, 1H, *p*-ArH), 7.30 (t, $^3J_{HH}$ = 7.8 Hz, 2H, *m*-ArH), 7.50 (d, $^3J_{HH}$ = 7.5 Hz, 2H, *o*-ArH) ppm. ^{13}C NMR (75.5 MHz, C$_6$D$_6$): 23.4 (CMe$_2$), 39.0 (NMe$_2$), 59.5 (ArCMe$_2$), 126.1 (*p*-/*m*-ArC), 127.9 (*o*-ArC), 148.7 (*ipso*-ArC) ppm.

Li(cuda): To a solution of cumyl-*N,N*-dimethylamine (4.0 g, 25 mmol) in 40 mL hexane, *tert*-BuLi (21 mL, 1.5 M in hexane, 32 mmol, 1.3 equiv.) was added in one portion at room temperature. The color of the reaction mixture changed *via* yellow into orange. The reaction mixture was stirred for 48 h, whereupon a colorless crystalline precipitate formed. It was filtered off and dried in vacuum. Compound was obtained as colorless solid in yield of 55% (2.3 g). Crystallization from ether yields Li(cuda) × ½Et$_2$O. ^{1}H NMR (300.1 MHz, C$_6$D$_6$): 1.34 (s, 6H, CMe$_2$), 1.68 (s, 6H, NMe$_2$), 7.16 (m, 3H,
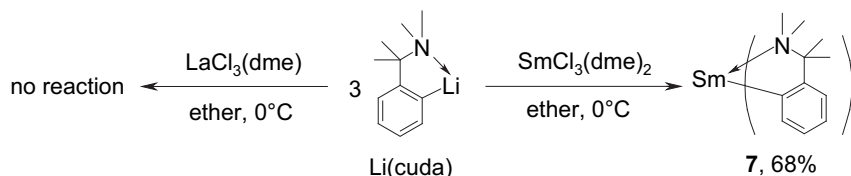
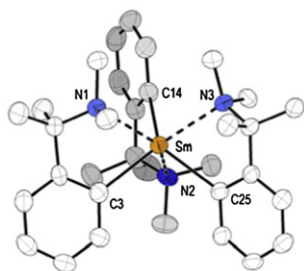**Scheme 8.** Reactivity of Li(cuda) with early and middle rare-earth metal halides.

Fig. 6. The molecular structure of complex [Sm(cuda)$_3$] (**7**). All hydrogen atoms have been omitted for clarity. Selected bond lengths (Å) and angles (°): Sm–C3 2.489(5), Sm–C14 2.528(5), Sm–C25 2.550(4), Sm–N1 2.710(4), Sm–N2 2.628(3) Sm–N3 2.709 (3); C3–Sm–C14 117.6(2), C14–Sm–C25 136.0(2), C25–Sm–C3 99.4(2), N1–Sm–N2 136.1(1), N2–Sm–N3 119.0(1), N3–Sm–N1 97.6(1); $\sum$(C$_A$–Sm–C$_B$) 353.0(6), $\sum$(N$_A$–Sm–N$_B$) 352.7(3); Sm···CCC 0.374(1), Sm···NNN 0.402(1).

m-/p-ArH), 8.22 (d, $^3J_{HH}$ = 5.5 Hz, 1H, o-ArH) ppm. Data for Li (cuda) × ½Et$_2$O: ^{1}H NMR (300.1 MHz, C$_6$D$_6$): 0.92 (t, $^3J_{HH}$ = 7.0 Hz, 3H, Et$_2$O), 1.42 (s, br, 6H, CMe$_2$), 1.76 (s, br, 6H, NMe$_2$), 3.14 (q, $^3J_{HH}$ = 7.0 Hz, 2H, Et$_2$O), 7.27 (m, 3H, m-/p-ArH), 8.26 (m, 1H, o-ArH) ppm. ^{13}C NMR (75.5 MHz, C$_6$D$_6$): 23.5 (s, br, CMe$_2$), 38.3 (NMe$_2$), 63.4 (CMe$_2$), 122.3, 125.0, 125.6 (ArC), 140.5 (ipso-ArC), 161.1 (ArC), 178.4 (ArC$_{Li}$) ppm. Anal. Calcd. for C$_{11}$H$_{16}$NLi: C 78.07, H 9.53, N 8.28. Found: C 78.75, H 9.33, N 8.54.

[(tmba)$_2$Lu(μ-Cl)]$_2$ (1). To a stirred suspension of [LuCl$_3$(thf)$_3$] (498 mg, 1.00 mmol) in ether (20 mL), solid Li(tmba) (310 mg, 2.00 mmol) was slowly added at room temperature. The reaction mixture was stirred for 0.5 h and the solvent was removed under reduced pressure. Toluene (10 mL) was added and resulting suspension was filtered through a Celite$^®$-pad and washed twice with the same solvent (2 × 5 mL). After removal of the solvent in vacuum, a foamy residue was crystallized from ether at −30 °C to yield a colorless crystalline solid (380 mg, 75%). ^{1}H NMR (300.1 MHz, C$_6$D$_6$): 1.30 (d, $^3J_{HH}$ = 6.7 Hz, 3H, CHMe), 2.01, 2.64 (2 × s, 2 × 3H, (Me)NMe), 2.98 (q, $^3J_{HH}$ = 6.7 Hz, 1H, CHMe), 6.92 (d, $^3J_{HH}$ = 7.4 Hz, 1H, ArH), 7.13–1.24 (m, 1H, ArH), 7.35 (t, $^3J_{HH}$ = 6.7 Hz, 1H, ArH), 8.25 (d, $^3J_{HH}$ = 6.6 Hz, 1H, o-ArH) ppm. ^{13}C NMR (75.5 MHz, C$_6$D$_6$): 25.4 (CHMe), 45.1, 45.3 ((Me)NMe), 74.7 (CHMe), 124.6, 125.1, 126.5, 139.8 (ArC), 154.9 (ipso-ArC), 192.3 (ArC$_{Lu}$) ppm. Anal. Calcd for C$_{20}$H$_{28}$ClLuN$_2$: C 47.39, H 5.57, N 5.53. Found: C 44.10, H 5.41, N 5.19.

[(tmba)$_2$Y(μ-Cl)]$_2$ (2). Similar procedure as in the synthesis of **1**, starting from [YCl$_3$(dme)$_2$] (375 mg, 1.00 mmol), Li(tmba) (310 mg, 2.00 mmol) in ether (20 mL). A colorless, analytically pure complex was isolated by crystallization at −30 °C from hexane in yield of 56%. Crystallization from ether affords the compound with composition [(tmba)$_2$Y(μ-Cl)] × 1.33Et$_2$O ^{1}H NMR (300.1 MHz,

C$_6$D$_6$): 1.30 (d, $^3J_{HH}$ = 6.4 Hz, 1H, CHMe), 2.04, 2.60 (2 × s, 2 × 3H, (Me)NMe), 2.86 (q, 1H, $^3J_{HH}$ = 6.4 Hz, CHMe), 6.87 (d, $^3J_{HH}$ = 7.3 Hz, 1H, ArH), 7.30 (t, $^3J_{HH}$ = 6.6 Hz, 1H, ArH), 8.16 (d, $^3J_{HH}$ = 6.3 Hz, 1H, o-ArH) ppm. ^{13}C NMR (75.5 MHz, C$_6$D$_6$): 26.1 (CHMe), 44.7, 44.9 ((Me) NMe), 74.7 (CHMe), 124.3, 124.9, 126.6, 138.3 (ArC), 154.3 (ipso-ArC), 183.14 (d, $^1J_{YC}$ = 48 Hz, ArC$_Y$,) ppm. Anal. Calcd for C$_{20}$H$_{28}$ClYN$_2$: C 57.08, H 6.71, N 6.66. Found: C 54.04, H 6.61, N 6.34.

[Y(tmba)$_3$] (3). Similar procedure as in the synthesis of **1**, starting from [YCl$_3$(dme)$_2$] (1.40 g, 3.70 mmol), Li(tmba) (1.75 g, 11.3 mmol) in ether (40 mL). The toluene extract was concentrated in vacuum to a volume of 2–3 mL. Upon addition of hexane (50 mL), a colorless solid precipitates. It was collected by filtration, washed with hexane (2 × 10 mL) and dried in vacuo. A colorless, microcrystalline solid was obtained in 78% of yield. ^{1}H NMR (300.1 MHz, C$_6$D$_6$): 1.13 (d br, $^3J_{HH}$ = 6.5 Hz, 3H, CHMe), 2.22 (s br, 6H, NMe$_2$), 3.16 (s br, 1H, CHMe), 6.97 (d, $^3J_{HH}$ = 7.5 Hz, 1H, m-ArH), 7.11 (dt, $^3J_{HH}$ = 1.2 Hz, $^3J_{HH}$ = 7.4 Hz, 1H, p-ArH), 7.20 (t, $^3J_{HH}$ = 7.2 Hz, 1H, m-ArH), 8.18 (s br, 1H, o-ArH) ppm. ^{13}C NMR (75.5 MHz, C$_6$D$_6$): 22.1 (s br, CHMe), 45.0 (s br, NMe$_2$), 73.5 (s br, CHMe), 124.2, 124.9, 125.8, 138.8 (ArC), 153.9 (s br, ipso-ArC), 185.9 (d, $^1J_{CY}$ = 44 Hz, ArC$_Y$) ppm. Anal. Calcd for C$_{30}$H$_{42}$N$_3$Y: C 67.53, H 7.93, N 7.88. Found: C 66.51, H 7.94, N 7.67.

[Dy(tmba)$_3$] (4). Similar procedure as in the synthesis of **1**, starting from [DyCl$_3$(dme)$_2$] (821 mg, 1.83 mmol) and Li(tmba) (853 mg, 5.48 mmol). Crystallization from hot hexane (20 mL) yields a yellowish, microcrystalline solid in yield of 83%. Anal. Calcd for C$_{30}$H$_{42}$N$_3$Dy: C 59.34, H 6.97, N 6.92. Found: C 58.23, H 7.12, N 6.45.

[Nd(tmba)$_3$] (5). To a stirred suspension of [NdCl$_3$(dme)] (681 mg, 2.00 mmol) in ether (20 mL), suspension of Li(tmba) (929 mg, 6.0 mmol) in toluene (10 mL) was gradually added at 0 °C. The reaction mixture was stirred for 0.5 h after that it was concentrated in vacuum to the one half of the original volume. The precipitated LiCl was filtered off through Celite$^©$ and washed with toluene (5 mL) to yield pale blue solution. All volatiles were removed in vacuum followed by hexane (10 mL) addition, whereupon a pale blue, heavy precipitate forms. It was isolated by filtration and was dried in vacuum. Complex was obtained as a pale blue, microcrystalline solid in 28% yield. Anal. Calcd for C$_{30}$H$_{42}$N$_3$Nd: C 61.18, H 7.19, N 7.13. Found: C 58.91, H 7.00, N 6.84.

[Sm(tmba)$_3$] (6). Similar procedure as in the synthesis of **5**, starting from [SmCl$_3$(dme)$_2$] (873 mg, 2.00 mmol) and Li(tmba) (931 mg, 6.00 mmol). A yellow, crystalline solid was obtained in 56% yield. Anal. Calcd for C$_{30}$H$_{42}$N$_3$Sm: C 60.55, H 7.11, N 7.06. Found: C 57.72, H 6.51, N 7.89.

An attempt of [La(cuda)$_3$] synthesis. To a stirred suspension of [LaCl$_3$(dme)] (335 mg, 1.00 mmol) in ether (20 mL), Li(cuda) (500 mg, 2.95 mmol) was added in portions at 0 °C. The suspension was stirred for additional 4 h at room temperature, the off-white

Table 3
Stability range of homoleptic aryl complexes of the rare earth metals as a function of the ortho-metallated benzylamine type.

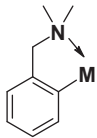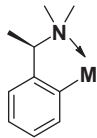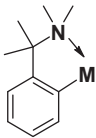|	M(dmba)$_3$	M(tmba)$_3$	M(cuda)$_3$
Early lanthanides (Ce–Sm and La)	Unstable for Ce–Sm	Fairly stable for Nd and Sm	Stable for Sm
Middle lanthanides (Eu–Ho and Y)	Unstable for Gd, Tb, Dy stable for Y only	Stable for Y and Dy also [Ar$_2$YCl]$_2$ stable	Unverified
Late lanthanides (Er–Lu and Sc)	Stable for Er, Yb and Lu	Unverified; only [Ar$_2$LuCl]$_2$ stable	Improbable

Table 4
Crystallographic data for **1**, **2***1.33(Et$_2$O), **3**, **4**, **5**, **8** and Li$_2$(cuda)$_2$, (Et$_2$O)$_{0.68}$, (dme)$_{0.32}$.

	(**1**)	(**2**)*1.33(Et$_2$O)	(**3**)	(**4**)	(**5**)	(**7**)	Li$_2$(cuda)$_2$, (Et$_2$O)$_{0.68}$, (dme)$_{0.32}$
Empirical formula	C$_{40}$H$_{56}$Cl$_2$Lu$_2$N$_4$	C$_{40}$H$_{56}$Cl$_2$N$_4$Y$_2$, 1.33(Et$_2$O)	C$_{30}$H$_{42}$N$_3$Y	C$_{30}$H$_{42}$DyN$_3$	C$_{30}$H$_{42}$N$_3$Nd	C$_{33}$H$_{48}$N$_3$Sm	C$_{26}$H$_{42}$Li$_2$N$_2$O$_{1.32}$
Crystal habit	Prism	Plate	Prism	Plate	Prism	Needle	Prism
Crystal colour	Colourless	Colourless	Colourless	Colourless	Colourless	Colourless	Colourless
Crystal size (mm)	0.15 × 0.12 × 0.12	0.33 × 0.24 × 0.06	0.3 × 0.2 × 0.1	0.18 × 0.09 × 0.03	0.27 × 0.27 × 0.17	0.27 × 0.06 × 0.01	0.30 × 0.24 × 0.21
Crystal system	Orthorhombic	Cubic	Monoclinic	Orthorhombic	Orthorhombic	Monoclinic	Monoclinic
Space group	P2$_1$2$_1$2$_1$	I 23	P2$_1$	P2$_1$2$_1$2$_1$	P2$_1$2$_1$2$_1$	P2$_1$/c	P2$_1$/c
Z	16	6	4	8	4	4	4
a (Å)	21.5996(3)	20.4405(8)	10.3760(18)	9.1297(6)	10.4845(9)	15.2069(10)	9.5086(7)
b (Å)	21.6102(3)		23.851(2)	22.055(6)	11.2139(10)	11.7296(6)	17.2830(19)
c (Å)	35.4648(7)		11.1035(9)	27.588(19)	23.7959(17)	17.1648(12)	16.2434(12)
β (°)			90.324(11)			90.816(6)	102.409(9)
Volume (Å^3)	16554.0(5)	8540.3(6)	2747.8(4)	5555(2)	2797.7(4)	3061.4(3)	2607.0(4)
θ range (°)	4.5–27.5	2.4–25.0	2–26	1.2–26	2.0–25.5	1.3–25	1.7–25
hkl ranges	−22 21, −14 28, −25 46	−22 6, −24 22, −15 24	−12 12, −29 28, −13 12	−11 11, −27 27, −31 33	−12 12, −13 13, −28 26	−18,18, −13, 13, −20, 20	−10 11, −20 20, −18 17
Flack parameter	−0.013(8)	−0.022(16)	−0.028(6)	0.011(14)	−0.017(18)		
Formula weight	1013.73	940.43	533.58	1214.33	588.91	637.09	417.62
μ(Mo Kα) (mm^{-1})	4.903	2.153	2.144	2.712	1.877	1.943	0.063
D_{calc} (g cm^{-3})	1.627	1.097	1.290	1.452	1.398	1.382	1.064
F(000)	8000	2952	1128	2472	1212	1316	914
Diffractometer type	IPDS-2T	IPDS2	IPDS1	IPDS2	IPDS1	IPDS2	IPDS1
T, K	100(2)	100(2)	193(2)	100(2)	193(2)	100(2)	193(2)
N	56,155	4453	18,697	33,898	16,292	38,844	15,880
N_{ind}	32733 [R_{int} = 0.0476]	2141 [R_{int} = 0.0578]	10212 [R_{int} = 0.0548]	9998 [R_{int} = 0.0837]	5150 [R_{int} = 0.0315]	5388 [R(int) = 0.1007]	4341 [R(int) = 0.0538]
N_{obs} [$I > 2\sigma(I)$]	30,255	1552	7027	6660	4755	3521	2379
N_{var}	1779	160	632	613	311	346	325
Abs. correction	Semi-empirical	Semi-empirical	None	Semi-empirical	Gaussian	Gaussian	None
T_{max}, T_{min}	0.5853, 0.4482	0.672, 0.6382		0.8205, 0.7068	0.7876, 0.6754	0.9588, 0.7367	
GoF (F^2)	1.041	0.958	0.848	0.727	1.002	0.818	0.799
$R_1(F)$, $wR_2(F^2)$	0.0389, 0.0881	0.0464, 0.1055	0.0417, 0.0746	0.0372, 0.0702	0.0291, 0.0699	0.0332, 0.0522	0.0377, 0.0840
Res. Extr. (e Å^{-3})	1.847, −1.924	0.447, −0.305	0.584, −0.589	0.776, −0.902	1.07, −0.952	0.492, −0.649	0.155, −0.121
Remarks	Twin matrix 0 1 0 1 0 0 0 0 −1 Ratio 58:42	Disordered ether, holes	Twin matrix 1 0 0 0 −1 0 0 0 −1 Ratio 62:38		Disorder of one ligand Ratio 60:40		Disorder Et$_2$O/dme Ratio 67:33

precipitate was filtered off through a Celite$^{©}$-pad and the solvent was gradually removed in vacuum to leave white microcrystalline precipitate. X-ray structure analysis of a single crystal picked out of thus obtained precipitate corresponded to the composition of [Li$_2$(cuda)$_2$(Et$_2$O)$_{0.68}$(dme)$_{0.32}$].

[Sm(cuda)$_3$] (7). To a stirred suspension of [SmCl$_3$(dme)$_2$] (437 mg, 1.00 mmol) in ether (20 mL), Li(cuda) (500 mg, 2.95 mmol) was added in portions at 0 °C. The bright yellow suspension formed immediately. It was stirred for additional 0.5 h at the same temperature. The LiCl formed was filtered off through a Celite$^{©}$-pad and the solvent was completely removed in vacuum leaving bright yellow foamy residue. Treatment with hexane (25 mL) causes dissolution of the foam and immediate precipitation of a lustrous bright yellow microcrystalline solid. It was filtered off and dried in vacuum. Compound is highly soluble in benzene, and methylcyclohexane rather than in hexane. It reacts irreversibly with THF under decomposition. Yield: 38 %. Anal. Calcd for C$_{33}$H$_{48}$N$_3$Sm: C 62.21, H 7.59, N 6.60. Found: C 61.18, H 7.92, N 6.49.

3.1. X-ray crystallographic studies

The structures of [Li$_2$(cuda)$_2$(Et$_2$O)$_{0.68}$(dme)$_{0.32}$], **1**–**5** and **7** were solved by direct methods and expanded by difference-Fourier syntheses using SHELX–97 software package. G. M. Sheldrick, Program for solution of crystal structures, SHELXS-97, Universität Göttingen, 1997; G. M. Sheldrick, Program for the refinement of crystal structures, SHELXL-97, Universität Göttingen, 1997. Program for the visualisation of structures, DIAMOND 3.2, Crystal Impact GbR, Bonn, Germany, 1997–2006; K. Brandenburg. Crystallographic data for all compounds are summarized in Table 4. CCDC reference numbers are CCDC 775561–775567. Atomic coordinates, bond lengths, bond angles and thermal parameters have been deposited at the Cambridge Crystallographic Data Centre (CCDC). These data can be obtained free of charge via www.ccdc.cam.uk/conts/retrieving.html (or from the CCDC, 12 Union Road, Cambridge CB2 1EZ, UK; fax: +44 1223 336 033; or deposit@ccdc.cam.ac.uk). Any request to the CCDC for data should quote the full literature citation and CCDC reference number.

Acknowledgements

Appendix A. Supplementary material

CCDC 775561–775567 contain the supplementary crystallographic data for this paper. These data can be obtained free of charge from The Cambridge Crystallographic Data Centre via www.ccdc.cam.ac.uk/data_request/cif.

References

[1] F.N. Jones, M.F. Zinn, C.R. Hauser, J. Org. Chem. 28 (1963) 663–665.
[2] A.L. Wayda, Organometallics 3 (1984) 939–941.
[3] L.E. Manzer, J. Am. Chem. Soc. 26 (1978) 8068–8073.
[4] M. Booij, N.H. Kiers, H.J. Heeres, J.H. Teuben, J. Organomet. Chem. 364 (1989) 79–86.
[5] A.R. Petrov, K.A. Rufanov, K. Harms, J. Sundermeyer, J. Organomet. Chem. 694 (2009) 1212–1218.
[6] (a) W.H. Puterbaugh, C.R. Hauser, J. Org. Chem. 28 (1963) 2467–2470;
(b) W.H. Puterbaugh, C.R. Hauser, J. Org. Chem. 28 (1963) 3465–3467.
[7] D. Hofmann, W. Bauer, F. Hampel, N.J.R. van Eikema Hommes, P.v.R. Schleyer, P. Otto, U. Pieper, D. Stalke, D.S. Wright, R. Snaith, J. Am. Chem. Soc. 116 (1994) 528–536.
[8] M. Westerhausen, W. Schwarz, Z. Naturforsch. B53 (1998) 625–627.
[9] F. Feil, S. Harder, Organometallics 19 (2000) 5010–5015.
[10] F. Feil, S. Harder, Organometallics 20 (2001) 4616–4622.
[11] D. Balderman, A. Kalir, Synthesis 1 (1978) 24–26.
[12] R.N. Icke, B.B. Wisegarver, G.A. Alles, Org. Synth. 25 (1945) 89–92.
[13] C.M.P. Kronenburg, E. Rijnberg, J.T.B.H. Jastrzebski, H. Kooijman, A.L. Spek, G. van Koten, Eur. J. Org. Chem. (2004) 153–159.
[14] C.M.P. Kronenburg, E. Rijnberg, J.T.B.H. Jastrzebski, H. Kooijman, M. Lutz, A.L. Spek, A. Gossage, G. van Koten, Chem. Eur. J. 11 (2005) 251–261.
[15] (a) M. Asakura, M. Oki, S. Toyota, Organometallics 19 (2000) 206–208;
(b) S. Toyota, M. Asakura, T. Futawaka, M. Oki, Bull. Chem. Soc. Jpn. 72 (1999) 1879–1885.
[16] In order to avoid ether cleavage side-reactions, THF was only allowed to be present as ligand at rare-earth metal halides of small ionic radius, such as Lu, Sc. DME adducts tend to be the better choice for rare-earth metal halides of middle and large ionic radii. In any case, working in ether as solvent (and not THF or DME) was essential for selective transformations and successful crystallisations.
[17] D. Cui, M. Nishiura, Z. Hou, Macromolecules 38 (2005) 4089–4095.
[18] C. Qian, W. Nie, J. Sun, Organometallics 19 (2000) 4134–4140.
[19] J. Sundermeyer, A. Petrov, O. Thomas, PCT Int. Pat. Appl. WO 2009/067999.
[20] G.W. Rabe, M. Zhang-Presse, F.A. Riederer, G.P.A. Yap, Inorg. Chem. 42 (2003) 3527–3533.
[21] W.J. Evans, I. Bloom, W.E. Hunter, J.L. Atwood, Organometallics 4 (1985) 112–119.
[22] N.S. Radu, S.L. Buchwald, B. Scott, C.J. Burns, Organometallics 15 (1996) 3913–3915.
[23] G.W. Rabe, M. Zhang-Presse, F.A. Riederer, J.A. Golen, C.D. Incarvito, A.L. Rheingold, Inorg. Chem. 42 (2003) 7587–7592.
[24] G.W. Rabe, B. Rhatigan, J.A. Golen, A.L. Rheingold, Acta Cryst. Sect. E E59 (2003) m99–m101.
[25] M. Niemeyer, S.-O. Hauber, Z. Anorg. Allg. Chem. 625 (1999) 137–140.
[26] U. Baisch, A. Dell, B. Daniela, F. Calderazzo, R. Conty, L. Labella, F. Marchetti, E.A. Quadrelli, Inorg. Chim. Acta 357 (2004) 1538–1548.